

Article citation info:

Šipoš M, Klaić Z, Nyarko K. E, Fekete K, A method for determining the location and type of fault in transmission network using neural networks and power quality monitors, *Eksploracja i Niezawodność – Maintenance and Reliability* 2024; 26(3) <http://doi.org/10.17531/ein/187166>

A method for determining the location and type of fault in transmission network using neural networks and power quality monitors

Indexed by:



Mario Šipoš^a, Zvonimir Klaić^{b,*}, Karlo Emmanuel Nyarko^b, Krešimir Fekete^b

^a Croatian Armed Forces, Croatia

^b Faculty of Electrical Engineering, Computer Science and Information Technology Osijek, Croatia., Croatia

Highlights

- The paper proposes a new procedure using neural networks to determine the location of a fault on a power line.
- The procedure involves four stages, three of which employ neural networks.
- The procedure was tested on the IEEE 39 bus transmission system using the DIgSILENT PowerFactory software.

Abstract

In this paper, a procedure for determining the location of a fault on a power line using neural networks is proposed. Specifically, the procedure involves four stages (three of which employ neural networks): gathering voltage input data from power quality monitors via simulation, classifying the fault type, detecting the faulted line, and determining the fault position on the power line. The IEEE 39 bus test system was used to develop and test the mentioned model. Input voltages are obtained using DigSILENT PowerFactory software in which a set of three-phase and single-phase short circuits are simulated. For the next steps of the method, voltages from all buses are not used, but only voltages from optimally placed power quality monitors on 12 buses in the IEEE 39 bus test system. In the second step, the first neural network is employed in order to classify the fault type – single-phase or three-phase. In the third stage, another neural network is used to determine the faulted line and in the fourth stage, the last neural network is developed to determine the fault position on the faulted line.

Keywords

neural networks, power quality, location of a fault, transmission system

This is an open access article under the CC BY license (<https://creativecommons.org/licenses/by/4.0/>)

1. Introduction

Today, thanks to improvements made in measurement devices and their communication capabilities with SCADA systems, the process of recording, analyzing, and learning of faults has become more streamlined, allowing operators to identify faults quickly throughout the network. Despite the assistance provided by fault data recorders in identifying faults, determining the precise location remains an arduous task. Traditional methods such as impedance-based techniques and traveling wave analysis have been employed for pinpointing fault locations.

However, those approaches are limited when the electricity distribution network experiences modifications due to factors like incorporating Distributed Generations (DGs), shifting loads, or modifying tap settings. An alternative method, the Adaptive Localizing Method (ALM), was proposed recently. ALM can overcome some drawbacks of current techniques and effectively deal with network variations, enabling accurate localization of faults [17].

In earlier days, the supervisory control and data acquisition

(*) Corresponding author.

E-mail addresses:

M. Šipoš mario.sipos86@gmail.com, Z. Klaić (ORCID: 0000-0002-7237-3565) zvonimir.klaic@ferit.hr, K. E. Nyarko (ORCID: 0000-0001-8041-3646) karlo.nyarko@ferit.hr, K. Fekete (ORCID: 0000-0002-3239-7618) kresimir.fekete@ferit.hr,

system (SCADA) was used primarily to observe the overall performance of the power system using data gathered by remote terminal units (RTU) [11] this approach offered only surface-level insights into the system's status. To obtain a deeper understanding of the system operations, the deployment of phasor measurement units (PMUs) facilitated advanced wide-area measurement systems (WAMS). PMUs collect vital data points, including voltage, current, and frequency, along with time stamps, utilizing GPS technology via a phasor data concentrator (PDC). Such sophisticated measurements allowed monitoring of the power system's steady-state and dynamic aspects. As a result, innovative wide-area fault location schemes were developed. While the previously discussed systems offer real-time monitoring data, identifying faults depends mainly on human expertise, which increases the likelihood of human error. Artificial Intelligence (AI) methods, specifically Machine Learning (ML), have emerged as alternatives for fault detection, classification, and localization owing to the shortcomings of traditional methods and limitations in deploying Phasor Measurement Units (PMUs). Machine Learning (ML) methods can work alongside SCADA and WAMS depending on whether the focus is on making online or offline decisions. Their capacity for rapid adaptation enables them to effortlessly recognize alterations within the grid's operating parameters and take corresponding actions. Utilizing pre-fault and post-fault current records allows ML algorithms to determine patterns that are indicators of potential faults [17].

The paper is organized as follows: Section 2 comprehensively describes the literature on neural networks employed for fault detection in electrical grids. Section 3, Theoretical Background on Voltage Sags. Section 4 describes the methodology used to simulate single-phase and three-phase short circuits in the IEEE 39 bus transmission system using DIgSILENT PowerFactory software. The study focused on simulating a specific transmission line, labeled line 26-29, for evaluating the accuracy of fault location detection methods. Section 5 presents the findings of the study based on the simulations performed using various neural network architectures and training datasets. The results showed that the proposed fault detection and classification methods achieved high accuracy rates. The report also highlights the importance of selecting the exemplary neural network architecture and

training dataset for optimal performance in real-world power grids.

2. Literature review

A novel method for identifying faults within electrical grids has been proposed by Xing et al. [18]. Their approach involved augmenting the traditional convolutional neural network image recognition algorithm ResNet, proposed by He et al. [7], with the improved Inception-ResNet model, enabling them to handle intricate images derived from modern smart grid technology efficiently. Moreover, they collected data on different types of faults, including single-phase, double-phase, two-phase, and triple-phase circuit faults taken from the IEEE39 bus system model. Furthermore, using a binary classification framework, they classified three-phase faults as simple and single-phase earth faults as complex. Simulation results showed that the improved Inception-ResNet model achieved better accuracy than other image classification algorithms based on deep learning.

Jiang et al. [8] introduced a novel solution for recognizing faults in electrical networks, which involves converting data acquired via Phasor Measurement Units (PMUs) into line graphs as input for the VGG convolutional neural network. By transforming PMU information into line graphs, changes over time become more evident, allowing for faster calculations and more effective fault detection. Researchers have constructed an electrical grid simulation model using DigSILENT software and written code in Python to gather and preserve phasor measurement unit (PMU) data corresponding to numerous faults. The result showed that line chart training can accurately classify symmetrical and unsymmetrical faults.

Orag et al. [13] have utilized artificial neural networks (ANN) to develop a novel technique for identifying and locating faults in electricity grids with high accuracy. They leveraged computer-simulated data in Matlab/Simulink from a 330-kV, 500-kilometer three-phase transmission line located in Nigeria to create realistic scenarios involving various types of faults, including single line-to-ground, double line-to-ground, and three-phase to-ground faults. By training the ANN algorithm on these synthesized datasets, they achieved perfect fault detection rates of 99.5% fault localization accuracy across diverse distances.

Fahim et al. [4] introduced an innovative Self-Attention Convolutional Neural Network (SAT-CNN) architecture for time series imaging-based feature extraction to enhance the accuracy of Transmission Line Fault Detection and Classification. A power system network 220 kV, 50 Hz grid with a total length of 100 km was modeled in Matlab. Experiments conducted in this setting showed promising results compared to existing models, highlighting the potential advantages of the proposed approach.

Li et al. [12] have introduced a new method for the real-time localization of faulted lines within a power grid network using Convolutional Neural Network technology. The proposed solution relies on collecting PMU measurements taken before and during a fault event from selected buses throughout the grid. Bus voltages act as inputs into a CNN classifier based on the AlexNet architecture, which can distinguish unique characteristics of each type of fault (three-phase short circuit, line to ground, double line to ground, or line-to-line fault) from simulated scenarios modeled using Power System Toolbox Matlab. After validation through testing on IEEE 39 and 68 bus system configurations, the method demonstrates strong performance in accurately determining the fault locations.

Han et al. [6] propose a new methodology for fault diagnosis in power systems by introducing novel preprocessing techniques involving gradient calculations and similarity assessments, leading to the creation of Visualized Similarity Images (VSIs) that enhance the performance of Convolutional Neural Networks (CNNs) used to identify transmission line faults in the system. The research evaluated the proposed

method through simulations of IEEE 24-bus power systems created in MATLAB/Simulink. Results indicate the proposed framework performs effectively with robust accuracy and tolerable sensitivity toward parameter settings.

Tokel et al. [16] developed a detection and classification system for faults within an electric power network based on artificial neural networks using Matlab's neural network toolkit. They tested their algorithm using simulations of the IEEE 13-bus test feeder run through the OpenDSS software, generating datasets representing regular operating states and fault conditions. Their findings indicated high success rates ranging from 99.4 percent to 99.8 percent across all fault categories when applying the system for diagnosis purposes.

3. Theoretical Background

Assessing the number of expected voltage sags and short interruptions at a particular location in the power system network during a specific period can be beneficial as these power quality issues have significant economic consequences.

The method of fault position is well-known for stochastic assessment of voltage sags induced by short circuits in large power systems. The method determines the probability density function of voltage dips due to short circuits in the network. The residual voltage on a given busbar (r) is expressed as a function of the moving fault node's (f) position (Figure 1). This results in a deterministic relation that connects two stochastic variables: fault position and residual voltage. The ultimate goal of the method is the cumulative frequency of events for a specific bus expression (1).

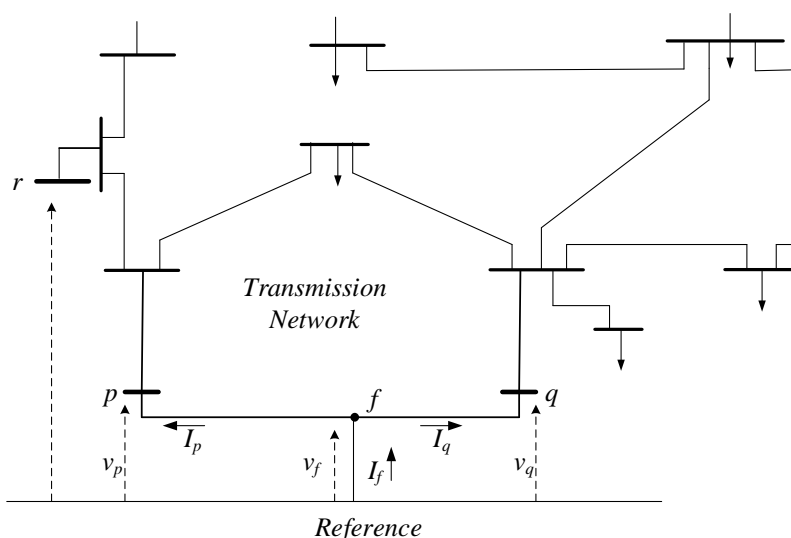


Fig. 1. Fault position between buses p and q .

$$F_v^m(v) = \sum_{Line=1}^{nLi} F_v(v) \quad (1)$$

In our research in [14], we applied the binary bat algorithm to identify the most suitable sites for placing voltage dip measuring devices and to determine the optimal number of such devices required to achieve maximum coverage at a minimal cost. It means that there are sufficient (optimally placed) voltage dip monitors to record every voltage dip in the test system due to any fault occurring anywhere in the test system. By improving the objective function (2), we utilized a Monitor Reach Area Matrix developed via short circuit simulations and the Exposed Coefficient to guide the algorithm toward its optimum solution. The optimal number of voltage dip measuring instruments for the IEEE 39 bus transmission system was twelve, and devices were placed on buses 12, 20, 25, 30 – 38.

$$Min \left(\sum_{i=1}^N x_i + \sum_{i=1}^N x_i \cdot k_i \right) \quad (2)$$

where x_i is the system bus (has a value of 0 or 1), and k_i is the weighted coefficient of the exposed area.

The research results in [14], the optimal number and placement of voltage dip monitors, gave us an idea and possibility for the next step: determining the location of the fault based on recorded voltage dips [15]. In [15], fault-affected lines were classified using the decision tree algorithm, giving accurate results. However, using multiple linear regression to determine the fault location at the line length did not give satisfactory results for all lines.

So, in this article, we use neural networks to determine the power system's fault position. From [14] we have the number and position of voltage dip monitoring devices in the IEEE 39 bus test system. The voltage values from the twelve buses during the voltage dip were used as input data for the neural network. These inputs are based on the changes in voltages measured during power system faults, expressed in per unit (p.u.) values.

4. Test model

This study focused on performing simulations of both three-phase and single-phase short circuits in the IEEE 39 bus transmission system using the DIgSILENT PowerFactory software. The simulation followed the standards specified by IEC 60909. The IEEE 39 bus system is modeled after New England's high voltage grid with four different voltage levels: 345 kV, 230 kV, 138 kV, and 16.5 kV. The system has ten generators, twelve transformers, 34 power lines, and nineteen load nodes [14]. Fig. 2. represents the IEEE 39 bus test system, where specific buses have been identified for installing voltage dip measurement devices. These devices are denoted by monitors displaying the corresponding bus numbers. Furthermore, a particular transmission line, labeled as Line 26-29, will serve as the testing ground for evaluating the accuracy of a fault location determination method along the transmission line length

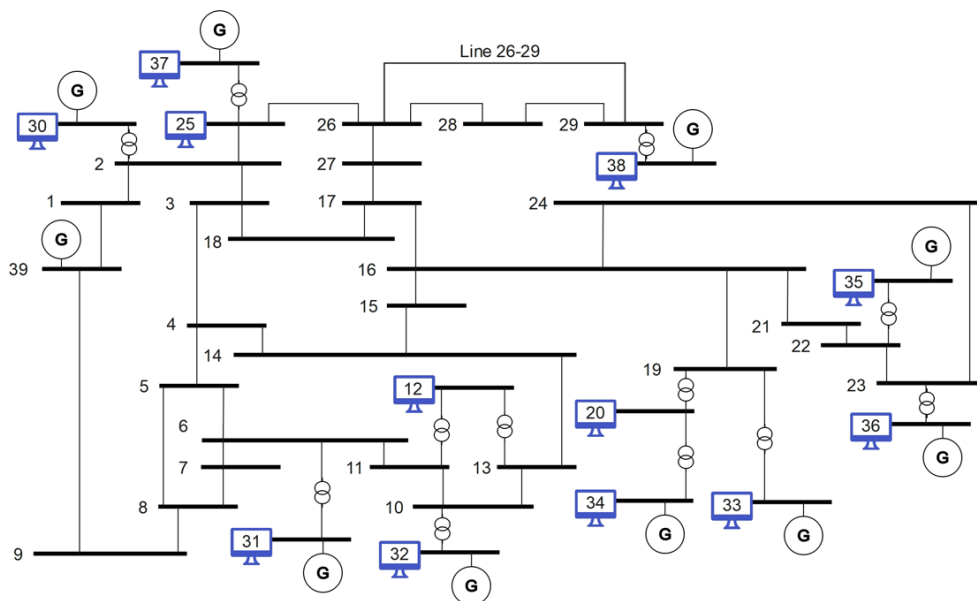


Fig. 2. The IEEE 39 bus test system.

5. Simulation results

The procedure for determining the fault position in the IEEE 39 bus test system consists of 4 steps and 3 neural networks, figure 3.

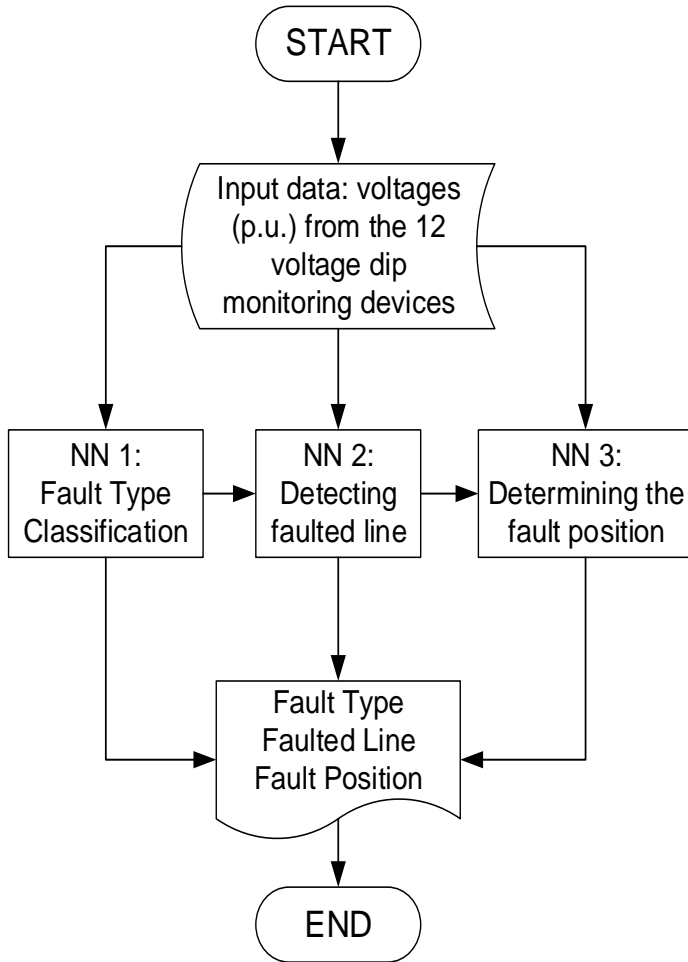


Fig. 3. The procedure for determining the fault position.

The fault detection process collects data from 12 buses in real time as input. Based on this input data and with the aid of the first neural network, the system then classifies the fault as either a three-phase or single-phase short circuit. After classifying the fault type, the second neural network is used to detect the line which is experiencing the fault. Depending on the detected line, the third neural network detects the fault position, whereby the result is given as a percentage of the line length. All three values, fault type, faulty line and fault position, are grouped together and shown on a display.

5.1. Input data: voltage values (p.u.) from the 12 voltage dip monitoring devices

Initially, it is necessary to simulate a three-phase or single-phase short circuit at an arbitrary location on the arbitrary power line

in the IEEE 39 bus test system. This simulation is performed using the DIgSILENT PowerFactory software. The short circuit simulation will cause changes in the voltages on busbars in the test system, which will be reflected in the voltages on the 12-voltage dip monitors. In every short-circuit simulation, voltage values were obtained on the power quality monitors that are optimally located on the 12 busbars of the system. Many sets of bus voltage values were used as input data for further steps of the proposed method (three neural networks).

5.2. Fault Type Classification

In this step, the type of fault is classified - whether it is a single line to ground or a three-phase fault. In multilayer neural networks, the number of neurons in the hidden layer is a crucial parameter that determines the capacity and complexity of the model. When selecting the appropriate number of neurons in the hidden layer, the complexity of the model, the computational efficiency and the ability to learn and generalize from the data must be weighed against each other. In this paper, we started with a single neuron in the hidden layer to train and test the network. Then we train the network again with the same training set, validation set and test set and increase the number of neurons in the hidden layer by one neuron. From the results obtained by simulation, we select the model with the lowest error (mean squared error) as that which defines the optimal number of neurons in the hidden layer to solve the given classification problem. This procedure was used to determine the optimal neural network structures for all three neural networks. For the fault type classification problem, the optimal number of neurons in the hidden layer was found to be 3.

The complete neural network structure for the fault type classification problem consists of three layers. The first layer or the input layer consists of 12 neurons. This number of neurons is determined by the number of inputs. The second or hidden layer consists of 3 neurons. This was determined by the aforementioned procedure. Finally, the final or output layer contains one neuron as the network's output. In the input layer, there are 12 p.u. voltage values on busbars obtained from voltage dip monitors during a single-phase and three-phase short circuit on the transmission line. The output layer of this neural network provides information as to whether a single-phase or three-phase short circuit has occurred. In this network,

we used the hyperbolic tangent (tanh) activation function (defined by Equation (3) and displayed in Fig. 4.) for the hidden layer and the sigmoid activation function (defined by Equation (4) and displayed in Fig. 5.) for the output layer.

$$f(x) = \tanh x = \frac{e^x - e^{-x}}{e^x + e^{-x}} \quad (3)$$

TanH is a type of nonlinear activation function that has a center point at 0, and its output values span the range from -1 to 1, as shown in Figure 4. Primarily employed within hidden layers, TanH aids in data centering because its mean is close to 0 or exactly 0. This property facilitates the learning process for subsequent layers [9]

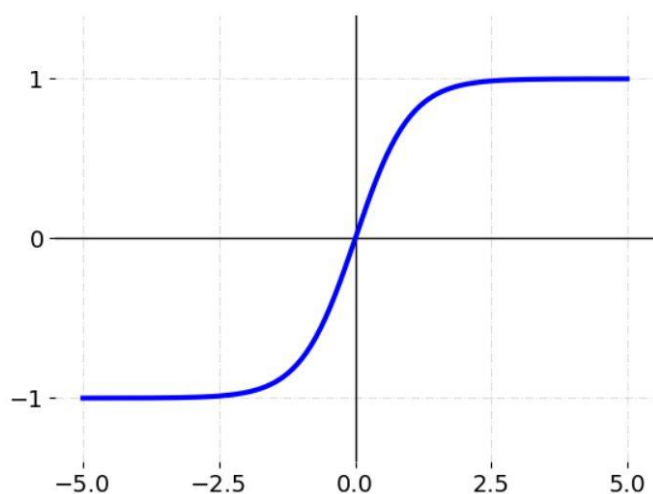


Fig. 4. Hyperbolic tangent activation function.

The utilization of the sigmoid activation function for the output layer in our model stems from the inherent requirement of performing binary classification, explicitly distinguishing between single-phase and three-phase short circuits.

The sigmoid activation function is a widely used activation function with broad applications. It can be mathematically expressed by equation (4).

$$f(x) = \frac{1}{1+e^{-x}} \quad (4)$$

The sigmoid function's graph is depicted in Fig. 5. When the input value, x , is small, the output of the sigmoid function approaches 0. Conversely, for larger x values, the output tends toward 1. By employing the sigmoid function, continuous real numbers are transformed into a range between 0 and 1. Consequently, this confines the input values of the subsequent layer within a fixed range, promoting more stable weight values [2].

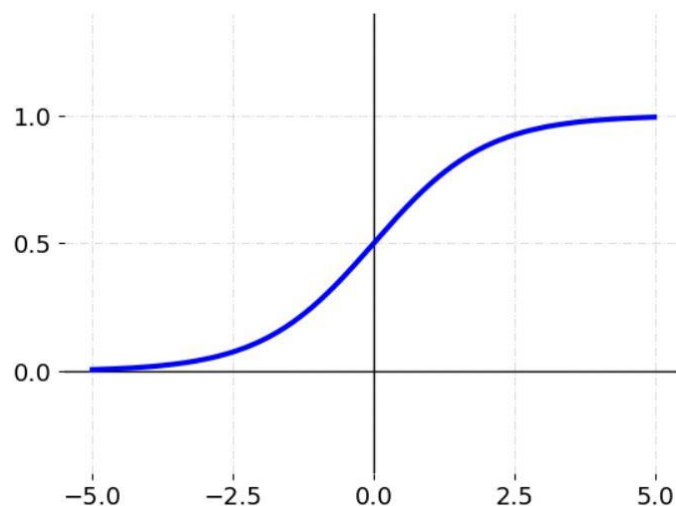


Fig. 5. sigmoid function.

There are 6696 examples in the dataset. Each example consists of 12 p.u. voltage values on the busbars during a short circuit on the transmission lines. Four thousand eighteen (4018) serve as training cases (60%), and the rest are divided into validation and testing sets, each having 1339 records (20% and 20%), respectively. The test set was then used to assess the effectiveness and accuracy of the trained network. By examining how well the trained network performed on unseen data, it became possible to evaluate its generalization abilities and understand if it could make accurate predictions outside its initial range of experience.

The confusion matrix is a commonly employed evaluation metric for addressing classification problems, suitable for binary and multiclass classification scenarios. Table 1. shows a confusion matrix specifically intended for binary classification.

Table 1. Confusion matrix specifically intended for binary classification.

	Predicted Positive	Predicted Negative
Actual Positive	True Positive (TP)	False Negative (FN)
Actual Negative	False Positive (FP)	True Negative (TN)

Regarding classification performance assessment, true positives (TP) correspond to instances where the algorithm correctly identifies positive outcomes based on the data. Conversely, false positives (FP) occur when the algorithm incorrectly labels negative outcomes as positive. False negatives (FN) refer to cases where the algorithm wrongly classifies positive outcomes as negative. True negatives (TN)

represent instances where the algorithm accurately recognizes negative outcomes.

The Confusion Matrix can be used to calculate performance metrics such as accuracy, precision, and Recall. It provides insight into how well the model performs by displaying the number of correctly classified examples against the total number of test samples from each label. Accuracy measures what percentage of all predictions were correct and is given by Equation (5). Accuracy is calculated as the sum of true positives, and true negatives divided by the sum of true positives, true negatives, false positives, and false negatives. The accuracy in a confusion matrix shows the proportion of correctly classified instances out of the total cases.

$$Accuracy = \frac{(TP + TN)}{(TP + TN + FP + FN)} \quad (5)$$

Precision calculates the proportion of true positive results compared to the total number of positive results and is defined by Equation (6). Precision is given by the number of true positives divided by the sum of true positives and false positives. Precision in a confusion matrix shows the ratio of true positive predictions to the total number of positive predictions.

$$Precision = \frac{TP}{(TP + FP)} \quad (6)$$

Recall calculates the proportion of correctly classified positives compared to the total number of actual positives (7). Recall is given by the number of true positives divided by the sum of true positives and false negatives. It shows the number of true positive predictions divided by the total number of actual positive instances.

$$Recall = \frac{TP}{(TP + FN)} \quad (7)$$

The different classes the model was trained upon are represented by the rows of the Confusion Matrix. Columns contain the outcome when using said prediction function. Each entry gives information about one class example. Summary stats can be found along diagonals where entries equal the number of ground truth matches for the corresponding row or column. The diagonal cells in the table show the number of correctly classified cases, and the off-diagonal cells show the misclassified cases [1].

For the current classification problem, the total number of test samples is 1339. The results obtained using the trained

neural network on the test set is displayed with the aid of a confusion matrix in Table 2. The number of correctly classified samples is 1339 (100.0%), and the number of misclassified samples is 0 (0.0%). There are no misclassified samples, so the neural network predicts this test data very well. The presented confusion matrix displays a classification of fault types. The total test sample shows 675 instances of single-line to-ground (1f) faults, accounting for 50.3% of the total.

Additionally, there are 665 occurrences of three-phase (3f) faults, representing 49.7% of the total sample. According to equations, Accuracy, Precision, and Recall are equal to 1 or 100% because there are no false positive and false negative values. Accuracy, precision, and recall need to be calculated separately for each class. In binary classification, the class receives the value 0 or 1. In our case, 0 represents a 1f fault, and 1 represents a 3f fault, where the value of 1f is the TP value in the confusion matrix, and 3f is the TN.

Table 2. Confusion matrix for single line to ground and three-phase fault classification.

	Predicted 1f	Predicted 3f	Total
Real 1f	674 (50,3%)	0 (0,0%)	674 (50,3%)
Real 3f	0 (0,0%)	665 (49,7%)	665 (49,7%)
Total	674 (50,3%)	665 (49,7%)	1339 (100%)

5.3. Detecting faulted line

In this study, the power network utilized is the IEEE 39 bus transmission system, which comprises 34 power lines. The identification of a defective power line is performed through a neural network application. This neural network consists of three layers: an input layer with twelve neurons, a hidden layer containing twenty-two neurons (determined using the aforementioned method in Subsection 5.2), and an output layer comprised of thirty-four neurons. The hyperbolic tangent activation function was chosen as the activation function within the model's hidden layers, while the softmax activation function was used for the output layer.

In multiclass classification challenges paired with cross-entropy loss, the softmax activation function is frequently utilized within the output layer. Its purpose is to scale the raw outputs generated by the preceding layer so that they sum up to 1. Usually, the previous layers generate an unscaled likelihood value for each class. Softmax modifies these values to generate

precise probabilities for each class membership option [10].

Multi-classification assignments usually benefit from conventional softmax classifiers due to their outstanding effectiveness. Normalizing diverse characteristics based on the number of classifications makes the positive elements more visible. Widely applied today, the softmax function frequently forms part of a loss function when working alongside the cross-entropy objective during classification [5].

The input layer of the neural network consists of 12 p.u. Voltage values were obtained from voltage dip monitors installed on busbars during a three-phase short circuit event on the transmission line. This data serves as the input to the network. On the other hand, the output layer of the neural network is responsible for providing information related to the faulted line, that is, the output neuron with the highest value (closest to one) indicates the line number where the fault is detected.

Of 3400 samples, 60%, 20%, and 20% are dedicated to training, validation, and testing. That is 2040, 680, and 680 samples. In the test data set, there are a total of 680 testing samples. After classification, it was observed that out of these samples, 98.7% were accurately categorized as per the given labels, while the remaining 1.3% were incorrectly classified. Specifically, 671 and 9 samples fell into the correct and misclassified categories.

When building a classification model, it is essential to know which of the samples are misclassified. This task involves identifying instances where the model has incorrectly categorized certain samples into classes they do not belong to. By doing so, we can better understand the strengths and weaknesses of our classifier and make improvements as needed. Neural networks learn patterns and relationships from the data they are trained on. If the training dataset does not adequately cover all possible fault scenarios or lacks sufficient examples of faults, the network may not generalize well to classify faults in that line correctly. Table 3 shows the misclassified lines.

Table 3. Misclassified lines.

Number	1	2	3	4	5	6	7	8	9
Real line in fault	L_7	L_10	L_10	L_14	L_23	L_32	L_32	L_33	L_33
Misclassified line	L_9	L_13	L_13	L_15	L_24	L_33	L_33	L_32	L_34

5.4. Determining the fault position on the power line

In this step, the location of the fault on the previously determined power line is determined by a neural network. The mentioned procedure was performed for Line 26-29.

Neural networks are adept at executing a mapping that approximates a function, which is acquired by learning from a provided collection of input-output value pairs. This learning process is commonly accomplished using the backpropagation algorithm [17].

The neural network consists of an input layer with 12 neurons, two hidden layers. The first consists of 3 neurons (determined arbitrarily), and the second consists of one neuron and an output layer of one neuron. In this model, the hyperbolic tangent activation function has been selected for the hidden layers, while the output layer employs the linear activation function. This activation function guarantees a derivative of 1 consistently due to using the function $f(x) = x$ [3]. The linear activation function is a simple activation function that outputs the input value without any transformation.

The input layer of the neural network comprises 12 p.u. voltage values acquired from measuring devices placed on busbars during a three-phase short circuit event on the transmission line. These voltage values serve as the input data for the network. On the other hand, the output layer of the neural network provides information regarding the position of the fault on the line length, expressed as a percentage ranging from 1 to 100%. For example, for a line 100 km long, a short circuit at 10% occurred on the tenth kilometer of the line as seen from the busbar with a lower number. Line 26-29 starts from busbar 26 (1%) and ends with busbar 29 (100%).

Fig 6. compares the predicted values by our neural network and the actual values for the output variable "Percent" – for Line 26-29. The output variable is the percentage value of the line length from 1% to 100% when viewed from the busbar with a smaller number. The grey line represents the ideal scenario where the predicted outputs perfectly align with the target values. The neural network randomly selects actual percent values for testing the neural network from the entire input data set of 100 data representing the length of the lines in Percent.

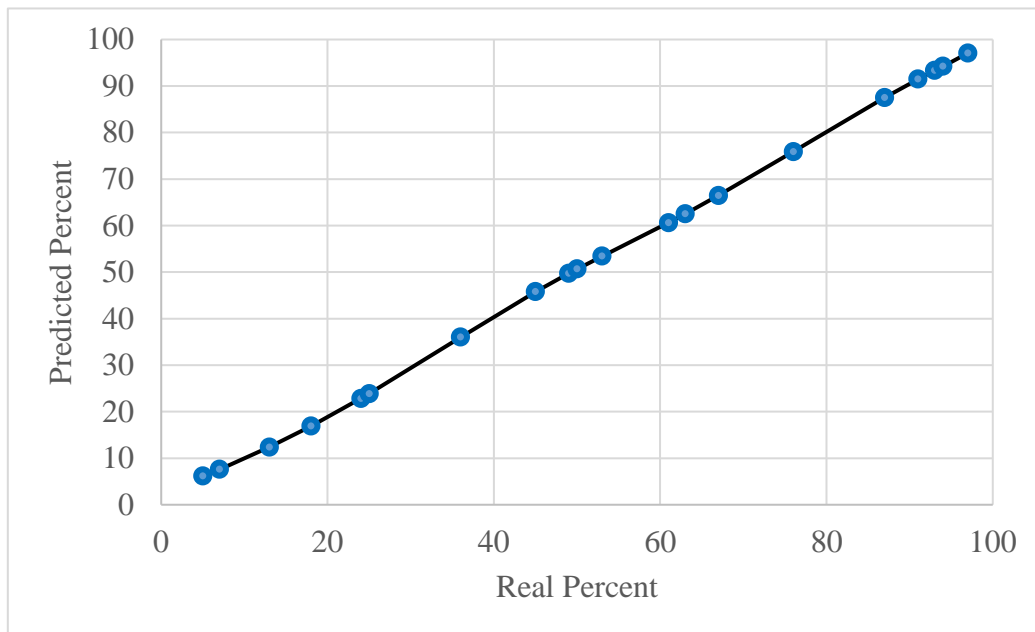


Fig. 6. Comparison between the predicted values and the actual values.

The table shows the actual percentage of the fault location on the length of the transmission line, the predicted percentage, and the difference between these two values.

The evaluated line in question was Line 26-29 of the IEEE 39 bus test system, spanning 247.96 kilometers. The selection of Line 26-29, provides a substantial line length for evaluating fault location methods. This choice allows for testing the methodology on a realistic transmission line that closely resembles the scale and complexity of actual power systems.

The smallest discrepancy was observed at 36% of the transmission line length, resulting in an error of merely 0.0228 %, equivalent to approximately 57 meters. Conversely, the most significant deviation occurred at the full 24 % transmission line length, with an error of 1.18%, corresponding to approximately 2.92 kilometers. It is important to emphasize here that for the classification of lines using this method, there must be a separate neural network for each line.

Table 4. IEEE 39 bus test system Line 26-29.

Real Percent [%]	Predicted Percent [%]	Difference [%]
5	6.127	1.127
7	7.57569	0.57569
13	12.3751	-0.6249
18	16.86	-1.14
24	22.8167	-1.1833
25	23.8633	-1.1367
36	36.0228	0.0228

Real Percent [%]	Predicted Percent [%]	Difference [%]
45	45.7875	0.7875
49	49.7272	0.7272
50	50.6718	0.6718
53	53.4129	0.4129
61	60.6192	-0.3808
63	62.4994	-0.5006
67	66.4472	-0.5528
76	75.898	-0.102
87	87.5107	0.5107
91	91.4785	0.4785
93	93.3374	0.3374
94	94.2257	0.2257
97	97.0824	0.0824

We conducted simulations utilizing various numbers of neurons within the hidden layer, ranging from 1 to 30 neurons (using the procedure mentioned in subsection 5.2). Among these configurations, the optimal outcome was achieved when employing 13 neurons in the first hidden layer.

The following table compares using 3 neurons in the hidden layer and the associated error in predicting the percentage of line length. A positive value in the last column indicates that the neural network with 13 neurons in the hidden layer exhibited a more significant error, whereas a negative value suggests that the network with 3 neurons in the hidden layer demonstrated a more significant error.

Upon examination, it becomes evident that in the event of

a fault occurring at 45% of the line length, the utilization of 13 neurons in the hidden layer results in an error reduction of 1382.78 meters compared to employing 3 neurons in the hidden

layer. However, in the case of a fault at 7% of the line length, implementing 13 neurons in the hidden layer leads to an error increase of 714.55 meters.

Table 5. Comparison of 13 neurons in the first hidden layer.

Real Percent [%]	Predicted Percent [%]	13 Neurons [%]	3 Neurons [%]	Error [m]
5	6.40	1.40	1.13	704.34
7	7.86	0.86	0.58	714.55
13	12.65	0.35	0.62	-699.52
18	17.12	0.88	1.14	-658.88
24	22.99	1.01	1.18	-443.23
25	24.01	0.99	1.14	-380.75
36	35.72	0.28	0.02	664.97
45	45.24	0.24	0.79	-1382.78
49	49.30	0.30	0.73	-1084.33
50	50.30	0.30	0.67	-955.80
53	53.23	0.23	0.41	-464.06
61	60.88	0.12	0.38	-670.81
63	62.79	0.21	0.50	-736.85
67	66.66	0.34	0.55	-550.67
76	75.80	0.20	0.10	239.52
87	87.48	0.48	0.51	-84.58
91	91.49	0.49	0.48	37.08
93	93.38	0.38	0.34	97.28
94	94.28	0.28	0.23	132.59
97	97.10	0.10	0.08	39.42

6. Conclusion

The paper proposed using multilayer neural networks to classify the fault in the power network, detect the faulty lines, and determine the place of fault that occurred along the length of the transmission lines of the IEEE 39 Bus test system. Three neural networks were used. The voltage values from the twelve busbars during the voltage dip were used as input data for the neural network. Each neural network has a different number of neurons in the hidden layer, which was determined by multiple simulations, and finally, the number of neurons with the lowest classification error was used. The results showed that neural networks could be used for the mentioned classification problems with accuracies of 100% for the classification of single-phase and three-phase short circuits and 98.7% for the

classification of faulty lines when tested on data that neural networks did not see before. Also, the neural network was able to determine the position of the fault on line length with an error ranging from 0,0228% to 1,9% in the location of the fault. When utilizing 13 neurons in the hidden layer, there is a significant reduction in error by 1382.78 meters compared to only three neurons in the hidden layer in the event of a fault occurring at 45% of the line length. In future research, we will focus on incorporating renewable energy sources, such as photovoltaic systems and wind farms, into the IEEE 39 bus test system. Subsequently, we aim to employ a neural network to discern the fault type and fault line in the transmission system while considering integrating renewable energy sources.

References

1. Batarseh F, Yang R, editors. *Data democracy: at the nexus of artificial intelligence, software development, and knowledge engineering*. London, United Kingdom: Academic Press, an Imprint of Elsevier; 2020. 241 p. <https://doi.org/10.1016/C2018-0-04003-7>
2. Chen Y, Li L, Li W, Guo Q, Du Z, Xu Z. *AI computing systems: an application driven perspective*. London: Morgan Kaufmann; 2024. 427 p.
3. Dangeti P. *Statistics for machine learning: techniques for exploring supervised, unsupervised, and reinforcement learning models with Python and R*. Birmingham, UK: Packt Publishing; 2017. 426 p.
4. Fahim SR, Sarker Y, Sarker SK, Sheikh MdRI, Das SK. Self attention convolutional neural network with time series imaging based feature extraction for transmission line fault detection and classification. *Electr Power Syst Res*. 2020 Oct 1;187:106437. doi:10.1016/j.epsr.2020.106437
5. Gao F, Li B, Chen L, Shang Z, Wei X, He C. A softmax classifier for high-precision classification of ultrasonic similar signals. *Ultrasonics*. 2021 Apr;112:106344. doi:10.1016/j.ultras.2020.106344
6. Han J, Miao S, Li Y, Yang W, Yin H. Fault Diagnosis of Power Systems Using Visualized Similarity Images and Improved Convolution Neural Networks. *IEEE Syst J*. 2022 Mar;16(1):185–96. doi:10.1109/JSYST.2021.3056536
7. He K, Zhang X, Ren S, Sun J. Deep Residual Learning for Image Recognition. In: 2016 IEEE Conference on Computer Vision and Pattern Recognition (CVPR). Las Vegas, NV, USA: IEEE; 2016. p. 770–8. doi:10.1109/CVPR.2016.90
8. Jiang L, Yi W. Power Grid Fault Diagnosis Method Based on VGG Network Line Graph Semantic Extraction. 2022;10(5). doi:SE22502172124
9. Jindal SK, Banerjee S, Patra R, Paul A. 9 - Deep learning-based brain malignant neoplasm classification using MRI image segmentation assisted by bias field correction and histogram equalization. In: Chaki J, editor. *Brain Tumor MRI Image Segmentation Using Deep Learning Techniques*. Academic Press; 2022. p. 135–61. doi:10.1016/B978-0-323-91171-9.00008-9
10. Ketkar N. *Deep Learning with Python*. Berkeley, CA: Apress; 2017. doi:10.1007/978-1-4842-2766-4
11. Kiio MN, Wekesa CW, Kamau SI. Development of electrical power transmission system linear hybrid state estimator based on circuit analysis techniques. *Heliyon*. 2022 Oct;8(10):e11000. doi:10.1016/j.heliyon.2022.e11000
12. Li W, Deka D, Chertkov M, Wang M. Real-Time Faulted Line Localization and PMU Placement in Power Systems Through Convolutional Neural Networks. *IEEE Trans Power Syst*. 2019 Nov;34(6):4640–51. doi:10.1109/TPWRS.2019.2917794
13. Ogar VN, Hussain S, Gamage KAA. The use of artificial neural network for low latency of fault detection and localisation in transmission line. *Heliyon*. 2023 Feb;9(2):e13376. doi:10.1016/j.heliyon.2023.e13376
14. Šipoš M, Klaić Z, Nyarko EK, Fekete K. Determining the Optimal Location and Number of Voltage Dip Monitoring Devices Using the Binary Bat Algorithm. *Energies*. 2021 Jan 5;14(1):1–13. doi:10.3390/en14010255
15. Sipos M, Klaić Z, Nyarko EK, Fekete K, Primorac M, Sljivac D. Determining the Fault Position in the Power System. In: 2020 International Conference on Smart Systems and Technologies (SST). Osijek, Croatia: IEEE; 2020. p. 135–9. doi:10.1109/SST49455.2020.9264078
16. Tokel HA, Halaseh RA, Alirezaei G, Mathar R. A new approach for machine learning-based fault detection and classification in power systems. In: 2018 IEEE Power & Energy Society Innovative Smart Grid Technologies Conference (ISGT). 2018. p. 1–5. doi:10.1109/ISGT.2018.8403343
17. Vaish R, Dwivedi UD, Tewari S, Tripathi SM. Machine learning applications in power system fault diagnosis: Research advancements and perspectives. *Eng Appl Artif Intell*. 2021 Nov 1;106:104504. doi:10.1016/j.engappai.2021.104504
18. Xing W, Zheng L, Bai J. Power Grid Fault Diagnosis Method Based on Improved Inception-ResNet Model Graph Semantic Extraction. *Int J Sci Eng Res IJSER*. 2020;9(8).